Feasibility of lattice radiotherapy using proton and carbon ion pencil beam for sinonasal adenoid cystic carcinoma

Dong Yang
Fudan University Shanghai Cancer Center https://orcid.org/0000-0001-9629-8945
Wei Wei Wang
Fudan University Shanghai Cancer Center
Ji Yi Hu
Fudan University Shanghai Cancer Center
Wei Xu Hu
Fudan University Shanghai Cancer Center
Xi Yu Zhang
Fudan University Shanghai Cancer Center
Xiao Dong Wu
Fudan University Shanghai Cancer Center
Jiade J Lu
Fudan University Shanghai Cancer Center
Lin Kong (lin.kong@sphic.org.cn)
Shanghai Proton and Heavy Ion Center, Fudan University Cancer Hospital https://orcid.org/0000-0003-4334-2484

Research

Keywords: Lattice radiotherapy, proton, carbon-ion, PBS, sinonasal ACC

Posted Date: January 25th, 2021

DOI: https://doi.org/10.21203/rs.3.rs-153143/v1

Feasibility of lattice radiotherapy using proton and carbon ion pencil beam for sinonasal adenoid cystic carcinoma

Dong Yang[a,b], Weiwei Wang[a,b], Jiyi Hu[b,c], Weixu Hu[b,c], Xiyu Zhang[a,b], Xiaodong Wu[a,b] , Jiade J Lu[b,c]* and Lin Kong[b,c,d]*

[a]Department of Medical Physics, Shanghai Proton and Heavy Ion Center, Fudan University Cancer Hospital, Shanghai, China; [b]Shanghai Engineering Research Center of Proton and Heavy Ion Radiation Therapy, Shanghai, China; [c]Department of Radiation Oncology, Shanghai Proton and Heavy Ion Center, Fudan University Cancer Hospital, Shanghai, China; [d]Department of Radiation Oncology, Shanghai Proton and Heavy Ion Center, Fudan University Shanghai Cancer Hospital, Shanghai, China

Jiade J Lu, Department of Radiation Oncology, Shanghai Proton and Heavy Ion Center, Fudan University Cancer Hospital, 4365 Kangxin Road, Pudong, Shanghai 201321, People's Republic of China, Email: jiade.lu@sphic.org.cn

Lin Kong, Department of Radiation Oncology, Shanghai Proton and Heavy Ion Center, Fudan University Cancer Hospital, 4365 Kangxin Road, Pudong, Shanghai 201321, People's Republic of China, Email: lin.kong@sphic.org.cn

Feasibility of lattice radiotherapy using proton and carbon ion pencil beam for sinonasal adenoid cystic carcinoma

Background: Adenoid cystic carcinomas (ACCs) are extremely rare, but they are a treatment challenge because they are highly radioresistant and are surrounded by several organs at risk (OARs). We aimed to investigate the feasibility of lattice radiotherapy (LRT) using pencil beam scanning (PBS) proton or carbon ion beams in the treatment of sinonasal ACC.

Patients and methods: Ten patients with nonoperative, bulky, and radioresistant ACCs were enrolled. Spherical vertices with a 1-cm diameter and average centre-to-centre distance of 3.51 cm were delineated within the gross tumour volumes. The prescription was 15 Gy (relative biological effectiveness [RBE]) to vertices and 3–3.5 Gy (RBE) to the periphery as clinical boost target volumes (CTVboosts) in one fraction. Photon, proton, and carbon-ion LRT plans were generated based on this. Peak-to-valley ratios (PVDRs) and dose delivered to the vertices, CTVboost, and OARs were compared among the three plans. The OAR doses were also compared between LRT plans and one fraction of clinical boost plans.

Results: The mean $PVDR_{min}$ for photon, proton, and carbon-ion LRT plans were 4.78 (range: 4.34–5.36), 4.82 (range: 4.15–5.37), and 4.69 (range: 4.31–5.28), respectively. The mean $PVDR_{mean}$ for

the same plans were 3.42 (range: 3.15–3.79), 2.93 (range: 2.19–3.74), and 3.58 (range: 3.09–4.68), respectively, with no significant differences in both. The brain stem, chiasm, optic nerve, parotids, spinal cord, and brain were better protected in proton and carbon-ion LRT plans than in photon LRT plans. Further, these plans did not introduce more doses to the OARs compared to the one-fraction clinical boost plan, with a significant difference.

Conclusion: Despite the minimal difference in PVDR between proton and carbon-ion LRT plans and photon LRT plans, the former can better protect OARs than photon LRT plans. Therefore, PBS proton and carbon-ion LRT can be used for sinonasal ACC.

Keywords: Lattice radiotherapy, proton, carbon-ion, PBS, sinonasal ACC

Background

Adenoid cystic carcinomas (ACCs) are extremely rare, accounting for 5% of all malignant sinonasal tumours and less than 0.15% of all malignancies of the head and neck[1-4]. ACCs are a treatment challenge as they are commonly diagnosed in the advanced stage due to the late occurrence of symptoms and their close proximity to important organs at risks (OARs). Further, ACCs are known to be radioresistant, and thus high doses are required for tumour control. Marginal misses or underdosing to the clinical targets in order to protect the OARs may cause local failure and recurrence[5-8] Therefore, reducing tumour radioresistance is key to ACC treatment.

Lattice radiotherapy (LRT) is a technique that delivers highly inhomogeneous doses to tumours, increasing apoptosis by bystander effects[9]. Furthermore, LRT can modify the immunosuppressive tumour environment, potentially enhancing the benefit of antigen-specific immunotherapy[10-11]. As such, LRT is a good candidate to increase the radiosensitivity of ACCs.

By using collimated photon beams, LRT can generate dose distributions concentrated in vertices while rapidly falling off outside the vertices. Clinical trials using photon LRT with an ARC delivery method for ovarian carcinosarcoma and non-small cell lung cancer have been conducted since 2015. These trials reported that LRT would result in a significant reduction in tumour size, thus helping to ensure a longer overall survival without severe OAR complications[12-15]. However, although these clinical trials have shown remarkable success, they still used a photon beam, which would deliver a high integral dose.

Proton and carbon ions delivered with a pencil beam scanning (PBS) technique can deposit Bragg peak to each vertex through inverse planning, thus delivering a high dose to the vertices while sharply decreasing the non-target doses. In addition, the scattering of proton beams is larger, resulting in carbon ion beams with a smaller full width at half maximum (FWHM). Less scattering may produce a higher peak-to-valley ratio (PVDR).

Gao et al[16] performed GRID therapy for deep and shallow targets using PBS proton beams, with a lateral space of 1.0 cm and 2.0 cm, in water phantoms. Based on these settings, they compared the dosimetric parameters between both PBS dose distributions and the typical photon GRID technique. They found that the proton GRID therapy provided higher PVDR than the photon GRID technique

for the deep-seated phantom target. Snider et al[17] delineated 3-dimensional spherical vertices with a diameter and centre-to-centre (c-t-c) of 3 mm and 3 cm, respectively. Based on the targets, they delivered mono-energetic proton PBS beams to the five tumours at different sites. The results showed that the peak dose could be achieved at 15 Gy (RBE) with a confluent valley dose across the targeted tumour of approximately 1–2 Gy (RBE). In addition, the skin could be safely protected.

This study aimed to investigate the feasibility of proton or carbon ion LRT plans for the treatment of ACCs. Towards this goal, the spherical vertices of 10 patients were delineated. The PVDR and doses to the periphery targets and OARs were compared among photon, proton, and carbon-ion LRT to determine whether proton and carbon-ion beams could promote the efficacy of LRT. The LRT plans were also compared to the clinical plans to determine whether LRT plans would increase the normal tissue complications.

Material and methods

Study design and patient selection

This retrospective study evaluated ten patients with ACCs who underwent biopsy and were treated with proton and carbon ion radiotherapy at the Shanghai Proton and Heavy Ion Center between 2015 and 2019. Only those with the largest tumour size were included. The tumour diameter ranged from 6.34 cm to 9.58 cm (mean: 8.02 cm) in the transverse view, corresponding to a gross tumour volume (GTV)

of 72.64–178.09 cc (mean 120.76 cc). None of the patients underwent surgery.

Treatment planning

Description of the lattice vertices

Based on the clinical contouring of OARs and targets, we additionally contoured the lattice vertices, which had a diameter of 1 cm, as suggested by Gholami et al[18]. All the vertices were in solid parts of the GTVs and were ensured to not overlap in the beam eye views to avoid high entrance doses. Two to three vertices were contoured per patient. The mean c-t-c (i.e. average distance between each vertex in the three dimensions) was 3.51 cm (range: 2.94–4.73 cm). Further, they were at least 1.6 cm apart and 1 cm away from any OAR. Figure 1 shows an example of vertices and the GTV of one patient.

Figure 1. An example of vertex geometry within the GTV.

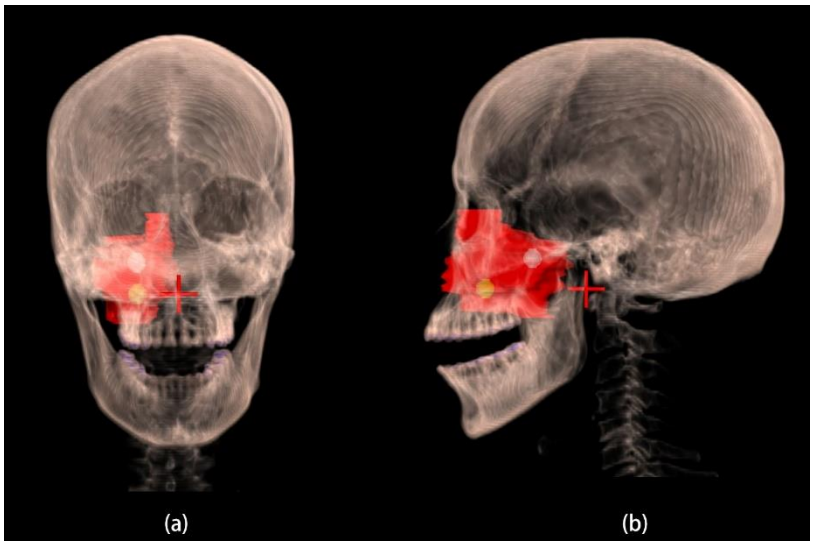

Notes: The GTV is 72.64 cc, 2 vertices were deployed with a c-to-c distance of 3.04 cm. (a) Patterns in coronal view. (b) Patterns in sagittal view.

Planning

For LRT, we prescribed 15 Gy (relative biological effectiveness [RBE]) to the vertices and 3–3.5 Gy (RBE) to the periphery as clinical boost target volumes (CTVboost) in one fraction. Proton and carbon ion LRT plans were generated using a 2–3 beam intensity-modulated proton (IMPT) and intensity-modulated carbon ion (IMCT) radiotherapy with a RayStation Treatment Planning System (TPS) (V10A, RaySearch Laboratories, Sweden). Photon LRT plans were generated using two full-field ARC radiotherapy in an Eclipse TPS (version V11; Varian Medical Systems, Palo Alto, CA, USA) with the same RT structures. The RBE of proton beams was constantly 1.1. The RBE of carbon ions was calculated using the local effect model I, as described by Krämer[19].

In general, patients receive 15–17.5 Gy (RBE) in 5 fractions of carbon ion radiotherapy to CTVboost as boost plans. In this study, the first fraction of the boost plan was replaced by our LRT plan. Therefore, we assumed that the patient received one fraction of the LRT plan and four fractions of the boost plans (LRT+boost). The OAR constraints for LRT plans were the same for all three modalities. The D_{max} for the brainstem was <1.5 Gy (RBE); chiasm, <0.6-3 Gy (RBE) (depending on the distance to CTVboost); optic nerves, <1–3 Gy (RBE); eyes, <1.8–2.6 Gy (RBE); lens, <1 Gy (RBE); skin, <5 Gy (RBE); and brain, <2.5 Gy (RBE). The patient characteristics and vertex details are listed in Table 1.

Table 1. Characteristics of the patients and vertices

Patient number	GTV (cc)	Diameter of GTV (cm)	Target depth (cm)	Number of Vertices	c-t-c distance (cm)	Vertex vol. (cc)
1	72.64	7.29	3.87	2	3.04	1.01
2	113.65	6.34	3.95	2	3.69	1.02
3	134.3	8.69	4.19	3	3.42	1.53
4	178.09	8.76	5.05	3	4.73	1.52
5	132.74	8.21	3.95	3	3.39	1.54
6	93.61	7.15	3.13	3	3.01	1.53
7	120.82	7.98	5.07	3	3.47	1.52
8	183.59	9.58	3.91	3	4.09	1.52
9	90.64	8.33	2.53	2	3.36	1.02
10	93.95	7.58	3.95	3	2.94	1.53

Abbreviations: GTV, gross tumour volume

Dose comparisons

The photon, proton, and carbon ion LRT plans were compared with respect to the peak-to-valley ratios (PVDRs), dose delivered to the OARs and vertices, and CTVboost. LRT plans were also compared to the one-fraction boost plans because the LRT plan should not increase the OAR toxicity.

The peak region was defined as the sum of all vertices. Amendola et al[15] delivered 18.00 Gy to vertices and 3.00 Gy to peripheral GTV using photon beams. The average dose falloff in their study from 18.00 Gy (100%) to 6.66 Gy

(37%) was 3.6 cm, which was more than the c-t-c distance in our study (i.e. 3.51 cm). Thus, our valley doses had to be higher than their criteria. Finally, we assumed that the valley dose was 7.5 Gy (50%) of the LRT prescription.

Accordingly, the valley region was derived as GTV minus vertices with a margin of 1 cm in the proton and carbon ion beam directions and 0.7 cm in other directions. We used 0.7 cm because the median distance from 50% isodose to the vertex boundary in the photon plans was 0.66 cm (range: 0.38–0.87 cm). Meanwhile, 1.0 cm was used due to the limitation of beam angles. Specifically, proton and carbon-ion LRT would have high entrance doses, with the carbon-ion LRT plan needing 1.18 cm (range: 0.22–4.61 cm) to lower the isodoses from 100% to 50%.

The PVDR was calculated using two methods. $PVDR_{min}$ was calculated based on the following (equation 1):

$$PVDR_{min} = \frac{D_{max}^{peak}}{D_{95}^{valley}} \quad (1)$$

where D_{max}^{peak} is the median D_{max} of each vertex, and D_{95}^{valley} is the dose covering 95% of the valley region, as is the semi-minimum dose of the valley region. The second method is shown in equation 2:

$$PVDR_{mean} = \frac{D_{mean}^{peak}}{D_{mean}^{valley}} \quad (2)$$

where D_{mean}^{valley} and D_{mean}^{peak} are the mean dose of the valley and peak region, respectively. It has been shown that high PVDRs and low valley doses can better spare normal tissues [20].

Several variables including D_{max} for the brain stem, chiasm, optic nerves, lens, spinal cord, skin, brain, and vertices; D_{mean} for the eyes, parotids, oral cavity and brain; and volume that received a minimum of 95% of the prescribed dose (V_{95}) for CTVboost were assessed for all three types of LRT plans. These parameters were also compared between one fraction of boost plans and LRT plans to determine whether LRT plans would induce potential OAR complications.

Statistical analysis

The PVDRs and doses to the vertices and targets of the three types of LRT plans were analysed using the SPSS 20.0 software (V20, IBM, America). Data between two types of plans were compared using the Wilcoxon rank-sum test. $P<0.05$ was considered statistically significant.

Results

Comparison of dose distribution

Figure 2 shows an example of dose distribution in photon, proton, and carbon ion LRT plans for one patient. The doses from the three LRT plans were distributed centrally in the vertices and lowered quickly outside the vertices.

Figure 2. Comparison of dose distributions among photon, proton, and carbon ion LRT plans.

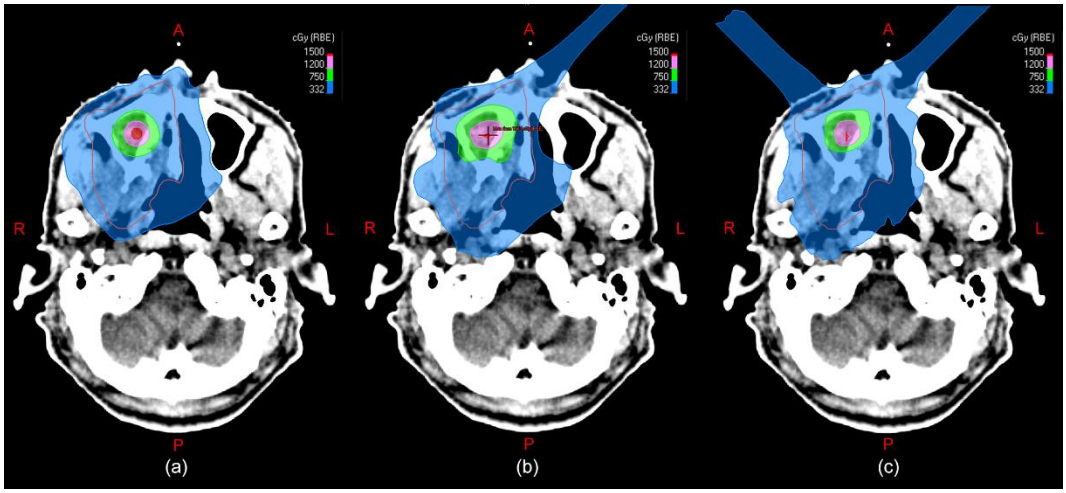

Notes: This patient has a GTV of 72.64 cc, 2 vertices, and 3.04 cm centre-to-centre distance. The prescribed dose of the LRT plan was 15 Gy (RBE) to the vertices and 3.5 Gy (RBE) in one fraction to the periphery as CTVboost. (a) Dose distribution of photon LRT plan. (b) Dose distribution of proton LRT plan. (c) Dose distribution of carbon ion LRT plan

PVDRs

The $PVDR_{min}$s and $PVDR_{mean}$s were compared between proton and carbon ion LRT plans and photon LRT plans (Figure 3). The mean $PVDR_{min}$ of the photon, proton, and carbon-ion LRT plans were 4.78 (range: 4.34–5.36), 4.82 (range: 4.15–5.37), and 4.69 (range: 4.31–5.28), respectively. Meanwhile, the mean $PVDR_{mean}$ for the same plans were 3.42 (range: 3.15–3.79), 2.93 (range: 2.19–3.74), and 3.58 (range: 3.09–4.68). The PVDRs showed no significant differences between photon, proton, and carbon-ion LRT plans: photon vs proton LRT plans: P=0.912 for $PVDR_{min}$ and P=0.063 for $PVDR_{mean}$; photon vs

carbon-ion LRT plans: P=0.436 for $PVDR_{min}$ and P=0.481 for $PVDR_{mean}$; and proton vs carbon-ion plans: P=0.436 for $PVDR_{min}$ and P=0.052 for $PVDR_{mean}$.

Figure 3. Comparison of $PVDR_{min}$ and $PVDR_{mean}$ among IMCT, IMPT, and photon ARC plans.

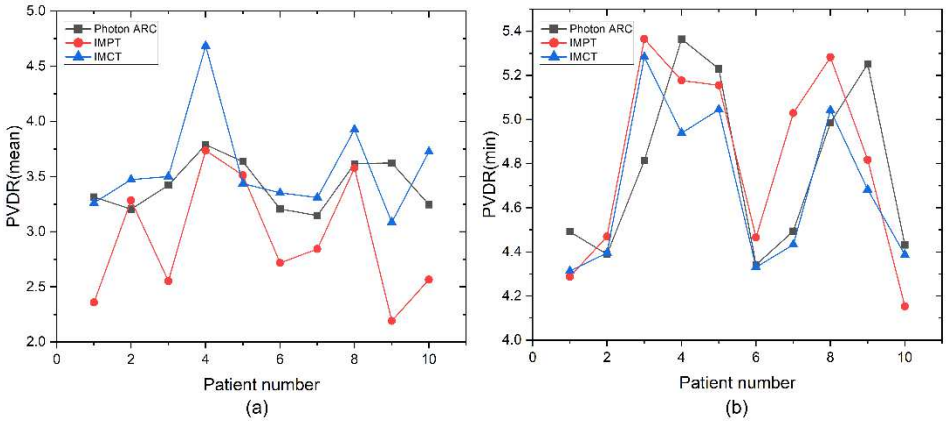

Notes: (a) Comparisons of $PVDR_{min}$; (b) Comparisons of $PVDR_{mean}$

Comparison among LRT plans and between one fraction of boost plans and LRT plans

The dose statistics of the variables from photon, proton, and carbon ion LRT plans are summarised in Table 2. There was no difference between proton and carbon-ion LRT plans, and they showed advantages over photon LRT plans in protecting the brain stem, chiasm, optic nerve, parotids, spinal cord, and brain. With respect to the dose to targets, photon LRT plans showed a higher V_{95} of CTVboost than proton LRT plans. Further, photon LRT plans showed the highest D_{max} of vertices among the three LRT plans.

Except for the D_{max} of the brain, there was no significant difference in the OAR dose and CTVboost dose between one fraction of boost plans and proton or

carbon-ion LRT plans. Meanwhile, the photon LRT plans would result in apparently higher doses to normal tissues. The results are shown in Table 3.

Table 3. Comparison of calculated doses between one fraction of LRT plans and one fraction of boost plans

		1 Fraction of boost plans	P-value		
			IMCT-boost	IMPT-boost	ARC-boost
Brain stem	D_{max}	1.19 (0.02–2.09)	0.337	0.142	0.002
Chiasm	D_{max}	1.74 (0.43–2.78)	0.096	0.289	0.000
Optic nerves	D_{max}	1.93 (0.87–3.00)	0.450	1.000	0.002
Lens	D_{max}	0.83 (0.05–1.54)	0.705	0.325	0.001
Left Parotid	D_{mean}	0.51 (0.03–1.85)	0.364	0.705	0.013
Right Parotid	D_{mean}	0.54 (0.01–1.58)	0.705	0.705	0.019
Spinal cord	D_{max}	0.30 (0.01–0.70)	0.241	0.120	0.000
Brain	D_{max}	3.52 (3.20–3.93)	0.009	0.041	0.048
	D_{mean}	0.19 (0.03–0.33)	0.337	0.142	0.002
Left Eye	D_{mean}	0.79 (0.08–1.66)	0.199	0.241	0.003
Right Eye	D_{mean}	0.60 (0.00–1.86)	0.307	0.496	0.006
CTVboost	V_{95}	97.40 (92.33–99.43)	0.529	0.075	0.579

Notes: 1 fraction of boost plans, 3–3.5 Gy (RBE) to CTVboost; LRT plans, 15 Gy (RBE) to vertices and 3–3.5 Gy (RBE) to CTVboost

Abbreviations: D_{max}, maximum dose; D_{mean}, mean dose; V_{95}, V_{95}, volume that received a minimum of 95% of the prescribed dose

Discussion

In this study, we delineated vertices for radioresistant ACC patients. Photon, proton and carbon-ion LRT plans were generated based on the vertices and peripheral target volumes. This is the first study to our knowledge to investigate the difference of dosimetry between photon, proton and carbon-ion LRT plans. Our results provide compelling evidence for proton and carbon-ion LRT as one fraction of boost treatment with 95% dose coverage of CTVboost and better protection of OARs than photon LRT plans.

Photon LRT has been performed in over 150 patients with advanced bulky tumours since its introduction in 2010 by Wu et al[21]. The LRT plans are used in combination with conventional radiotherapy or chemotherapy. LRT has been established as the main contributor to further reductions in tumour size and longer patient survival without significant morbidity or toxicity. Several studies have reported that PBS proton or carbon provides better dosimetry over photons. Thus, we performed a comparison study to characterise the potential benefits of proton and carbon-ion LRTs.

Creating localised high-dose islands and low-dose valleys within the tumour volumes is a basic principle of LRT. However, the dose to surrounding organs limits the use of LRT in current photon beam technologies. To overcome this limitation, proton and carbon-ion were introduced, but only proton-based

GRID therapy has been studied. However, the entrance dose in the proton GRID plan was high, and the beam angles were limited. Strongly grounded in GRID therapy, LRT can produce a highly concentrated dose distribution but with the added flexibility in three dimensions. This may reduce the entrance dose and maintain the conventional dose the surrounding OARs.

The characteristics of vertices in our study were set in reference to that in previous photon LRT cases, with diameters of approximately 1 cm and c-t-c of approximately 2–5 cm. Smaller vertex sizes and narrower separation are possible because the FWHM of proton and carbon ions are smaller than those of photons. Further research is needed to validate the optimal characteristics of the vertices in proton and carbon-ion LRT plans.

High PVDR is the key objective of successful LRT for large tumours. The small difference in PVDR among scattered photons, protons, and carbon ions is a result of the large PBS spot size caused by low energy when treating shallow tumours and the fewer fields in proton and carbon-ion plans than photon plans. This leads to the comparable PVDRs between photon, proton, and carbon-ion LRT plans. Concurrently, less lateral scattering of particle beams, especially carbon-ion beams, enables lower doses to the OARs in proton and carbon-ion plans.

LRT can be used to induce immune responses through its high-dose component, including abscopal effects and bystander effects. The presence of a bystander in GRID has been experimentally documented by a significant decrease in clonogenic survival and an increase in the expression of DNA damage genes in bystander cells[22-23]. Larger tumours may release more antigens in response to

irradiation, which potentially intensifies the abscopal effects[24]. Furthermore, the combination of radiation and immunotherapy can enhance T cell infiltration and inhibition of myeloid-derived suppressor cells and regulatory T cells[25]. As such, many factors, including the characteristics of vertices and radiation sequence, need to be further explored to augment the immunogenic responses.

Carbon-ion beams with high linear energy transfer values have been shown to possess higher RBE and induce more complex DNA damage. Importantly, they cause a significant reduction in radioresistance [26-30]. Meanwhile, carbon-ion beams may lead to radiation-induced bystander effects and abscopal effects in high-dose irradiation of partial tumours. These effects may be induced in a different manner as compared to that of photons, as reported in an animal model study[31]. However, the advantage of carbon-ion is yet to be investigated. We believe that it is imperative to conduct this dosimetric comparison and thus conducted it as part of this study.

Sinonasal ACC is a bulky tumour that is not tractable by conventional radiation due to the sensitive surrounding OARs. Moreover, the large hypoxic tumour volumes within the tumour may induce hypoxia, thus reducing apoptosis[9]. In contrast to conventional photon beam radiotherapy, LRT with carbon ions can better deliver high-dose radiation to the target tumour. Further, it can induce bystander effects and abscopal effects to increase apoptosis in the peripheral tumour cells while having no adverse effects on adjacent organs, as indicated in our study. Therefore, LRT with carbon ions is an advantageous option as one fraction of the boost plans to treat sinonasal ACCs.

This study has some limitations. The evaluation of LRT plans needs to take more factors into consideration, especially when combined with proton and carbon-ion beams. Range uncertainty is a main problem in particle radiotherapy. Due to the limited number of beams and the complicity of the patient's anatomy, this problem may be more severe. Therefore, the geometry design of the vertex and beam angle selection should be more cautious. In this study, LEM was used to calculate the RBE-weighted carbon-ion LRT. Whether this model can accurately predict the RBE of carbon ions at such a high dose level is still a question. Thus, the prescribed doses may not be clinically equivalent for the three modalities.

Conclusion

Dosimetric comparisons of photon, proton, and carbon-ion LRT plans showed no significant difference in PVDR. However, proton and carbon-ion LRT plans can protect the OARs better than photon LRT plans. This was also confirmed by comparing doses delivered to OARs and the GTV between one fraction of boost plans and LRT plans. Therefore, a prospective clinical study is warranted to evaluate the efficacy of proton or carbon-ion LRT plans for the treatment of ACCs, particularly in terms of tumour control and toxicity of normal tissues.

Declarations

Ethics approval and consent to participate

As a retrospective study, the work was approved by the Shanghai Proton and Heavy Ion Centre Institutional Review Board.

Consent for publication

Not applicable

Availability of data and materials

The datasets used and analysed during the current study are available from the corresponding author on reasonable request.

Competing interests

The authors declare that they have no competing interests.

Finding

This work was supported by the Program of Shanghai Academic/Technology Research Leader [18XD1423000].

Authors' contributions

YD designed and carried out the work, analysed data, and was a major contributor in writing the manuscript. WWW designed the work, analysed data, and substantively revised the manuscript. HJY and HWX designed the work, acquired,

and analysed data. ZXY and WXD analysed data. LJD and KL designed the work and revised the manuscript. All authors read and approved the final manuscript.

Acknowledgements

We greatly appreciate the generosity of Raysearch Company, who provided the treatment planning system (V10A, Raystation, Sweden).

References

1. Spiro RH, Huvos AG, Strong EW. Adenoid cystic carcinoma of salivary origin. A clinicopathologic study of 242 cases. American Journal of Surgery. 1974;128:512-520.
2. Michel G, Joubert M, Delemazure AS. Adenoid cystic carcinoma of the paranasal sinuses: Retrospective series and review of the literature. European Annals of Otorhinolaryngology-Head and Neck Disease. 2013;130:257–262.
3. Kim GE, Park HC, Keum KC, et al. Adenoid cystic carcinoma of the maxillary antrum. American Journal of Surgery. 1999;20:77-84.
4. Akbaba S, Ahmed D, Mock A, et al. Treatment Outcome of 227 Patients with Sinonasal Adenoid Cystic Carcinoma (ACC) after Intensity Modulated Radiotherapy and Active Raster-Scanning Carbon Ion Boost: A 10-Year Single-Center Experience. Cancers. 2019;11:1705.
5. Terhaard CH, Lubsen H, Rasch CR, et al. Neck Oncology Cooperative G: The role of radiotherapy in the treatment of malignant salivary gland tumors. Int. J. Radiat. Oncol. Biol. Phys. 2005;61:103-111.

6. Garden AS, Weber RS, Ang KK, et al. Postoperative radiation therapy for malignant tumors of minor salivary glands. Outcome and patterns of failure. Cancer. 1994;73:2563–2569.
7. Chen AM, Bucci MK, Weinberg V. Adenoid cystic carcinoma of the head and neck treated by surgery with or without postoperative radiation therapy: Prognostic features of recurrence. Int. J. Radiat. Oncol. Biol. Phys. 2006;66:152-159.
8. Geara FB, Sanguineti G, Tucker SL. Carcinoma of the nasopharynx treated by radiotherapy alone: Determinants of distant metastasis and survival. Radiother. Oncol. 1997;43:53-61.
9. Pellizzon ACA. Lattice radiation therapy – its concept and impact in the immunomodulation cancer treatment era[J]. Revista da Associao Médica Brasilra. 2020;66(6):728-731.
10. Asur R, Butterworth KT, Penagaricano JA, Prise KM, Griffin RJ. High dose bystander effects in spatially fractionated radiation therapy. Cancer Lett. 2015;356(1):52-57.
11. Yakovlev VA. Role of nitric oxide in the radiation-induced bystander effect. Redox Biol. 2015;6:396-400.
12. Amendola BE, Perez NC, Wu X, et al. Improved outcome of treating locally advanced lung cancer with the use of lattice radiotherapy (LRT): A case report. Clin Transl Radiat Oncol. 2018;9:68-71.
13. Amendola BE, Perez N, Amendola MA, et al. Lattice radiotherapy with RapidArc for treatment of gynecological tumors: Dosimetric and early clinical evaluations. Cureus. 2010;2:e15

14. Blanco Suarez JM, Amendola BE, Perez N, Amendola M,Wu X. The use of lattice radiation therapy (LRT) in the treatment of bulky tumors: A case report of a large metastatic mixed Mullerian ovarian tumor. Cureus. 2015;7:e389.
15. Amendola BE, Perez NC, Wu X, et al. Safety and Efficacy of Lattice Radiotherapy in Voluminous Non-small Cell Lung Cancer. Cureus. 2019;11(3).
16. Gao M, Mohiuddin MM, Hartsell WF, et al. Spatially Fractionated (GRID) Radiation Therapy using Proton Pencil Beam Scanning (PBS): Feasibility Study and Clinical Implementation[J]. Medical Physics. 2018;45(4):1645-1653.
17. Snider JW, Diwanji T, Langen KM. A Novel Method for the Delivery of 3-Dimensional High-Dose Spatially Fractionated Radiation Therapy with Pencil Beam Scanning Proton Therapy: Maximizing the Benefit of the Bragg Peak. International Journal of Radiation Oncology Biology Physics. 2017;99(2):S232-S233.
18. Gholami S, Nedaie HA, Longo F, et al. Grid block design based on Monte Carlo simulated dosimetry, the linear quadratic and Hug-Kellerer radiobiological models. J Med Phys. 2017;42(4):213-221
19. Krämer M, Scholz M. Treatment planning for heavy-ion radiotherapy: calculation and optimization of biologically effective dose. Phys Med Biol. 2000;45(11):3319-3330.
20. Zwicker RD, Meigooni A, Mohiuddin M. Therapeutic advantage of grid irradiation for large single fractions. Int J Radiat Oncol Biol Phys. 2004;58:1309-1315.

21. Wu X, Ahmed MM, Wright J, Gupta S, Pollack A. On modern technical approaches of three-dimensional high-dose Lattice radiotherapy (LRT). Cureus. 2010;2.
22. Asur R, Butterworth KT, Penagaricano JA, et al. High dose bystander effects in spatially fractionated radiation therapy. Cancer Lett. 2015;356:52–57.
23. Protopapa M, Kouloulias V, Kougioumtzopoulou A, et al. Novel treatment planning approaches to enhance the therapeutic ratio: targeting the molecular mechanisms of radiation therapy. Clinical and Translational Oncology. 2020;4(22):447-456.
24. Wang R, Zhou T, Liu W, et al. Molecular mechanism of bystander effects and related abscopal/cohort effects in cancer therapy. Cocotarget. 2018,9:18637-18647.
25. Persa E, Balogh A, Sáfrány G, Lumniczky K. The effect of ionizing radiation on regulatory T cells in health and disease. Cancer Lett. 2015;368(2):252-261.
26. Dokic I, Mairani A, Niklas M, et al. Next generation multi-scale biophysical characterization of high precision cancer particle radiotherapy using clinical proton, helium-, carbon- and oxygen ion beams. Oncotarget. 2016;7(35):56676-56689.
27. Klein C, Dokic I, Mairani A, et al. Overcoming hypoxia-induced tumor radioresistance in non-small cell lung cancer by targeting DNA-dependent protein kinase in combination with carbon ion irradiation. Radiat Oncol. 2017;12(1):208.

28. Valable S, Gerault AN, Lambert G, et al. Impact of Hypoxia on Carbon Ion Therapy in Glioblastoma Cells: Modulation by LET and Hypoxia-Dependent Genes. Cancer. 2020;12(8):2019.
29. Furusawa Y, Fukutsu K, Aoki M, et al. Inactivation of aerobic and hypoxic cells from three different cell lines by accelerated (3)He-, (12)C- and (20)Ne-ion beams. Radiat Res. 2000;154(5):485-496.
30. Tinganelli W, Ma NY, Von Neubeck C, et al. Influence of acute hypoxia and radiation quality on cell survival. J Radiat Res. 2013;54(Suppl 1):i23–30.
31. Huang Q, Sun Y, Wang W, et al. Biological Guided Carbon-Ion Microporous Radiation to Tumor Hypoxia Area Triggers Robust Abscopal Effects as Open Field Radiation. Frontiers in Oncology. 2020,10:597702.

Table 2. Dosimetric comparisons of OARs among the three types of LRT plans

[This table should be displayed on Page 12, Line 7]

		Photon ARC	IMPT	IMCT	P-value		
					ARC-IMPT	ARC-IMCT	IMPT-IMCT
Brain stem	D_{max}	2.52 (1.96–3.18)	0.88 (0.03–1.68)	0.75 (0.03–1.57)	0.000	0.000	0.596
Chiasm	D_{max}	2.61 (1.76–3.14)	1.61 (0.28–3.05)	1.59 (0.25–3.03)	0.016	0.009	0.821
Optic nerve	D_{max}	2.79 (2.29–3.15)	2.00 (0.83–3.00)	1.90 (0.92–2.95)	0.013	0.013	0.473
Lens	D_{max}	1.92 (0.91–3.14)	1.27 (0.02–2.76)	1.23 (0.02–2.82)	0.112	0.082	0.677
Left Parotid	D_{mean}	1.32 (0.79–2.85)	0.69 (0.01–2.02)	0.69 (0.07–1.84)	0.049	0.041	0.791
Right Parotid	D_{mean}	1.24 (0.59–1.81)	0.41 (0.00–1.03)	0.48 (0.04–1.04)	0.001	0.002	0.622

Spinal cord	D_{max}	1.55 (0.98–2.54)	0.15 (0.00–0.55)	0.15 (0.01–0.46)	0.000	0.000	0.705
Skin	D_{max}	4.31 (1.17–6.24)	4.35 (2.86–5.86)	4.74 (2.86–5.97)	0.734	0.199	0.307
Brain	D_{max}	4.21 (3.62–5.85)	2.85 (1.68–3.66)	2.69 (1.71–3.47)	0.006	0.002	0.406
	D_{mean}	0.77 (0.54–1.08)	0.31 (0.11–0.49)	0.28 (0.11–0.49)	0.002	0.002	0.608
CTVboost	V_{95} (%)	98.01 (92.53–99.96)	95.69 (90.49–99.13)	96.82 (90.37–99.85)	0.023	0.257	0.131
Vertices	D_{max}	16.28 (15.11–17.45)	16.10 (15.34–17.73)	15.58 (14.83–16.54)	0.019	0.015	0.247

Notes: ARC-IMPT, comparisons between photon ARC plans and IMPT plans; ARC-IMCT, comparisons between photon ARC plans and IMCT plans; IMPT-IMCT, comparisons between IMPT plans and IMCT plans

Abbreviations: D_{mean}, mean dose; D_{max}, maximum dose (point and/or in a significant volume), V_{95}, volume that received a minimum of 95% of the prescribed dose.

Figures

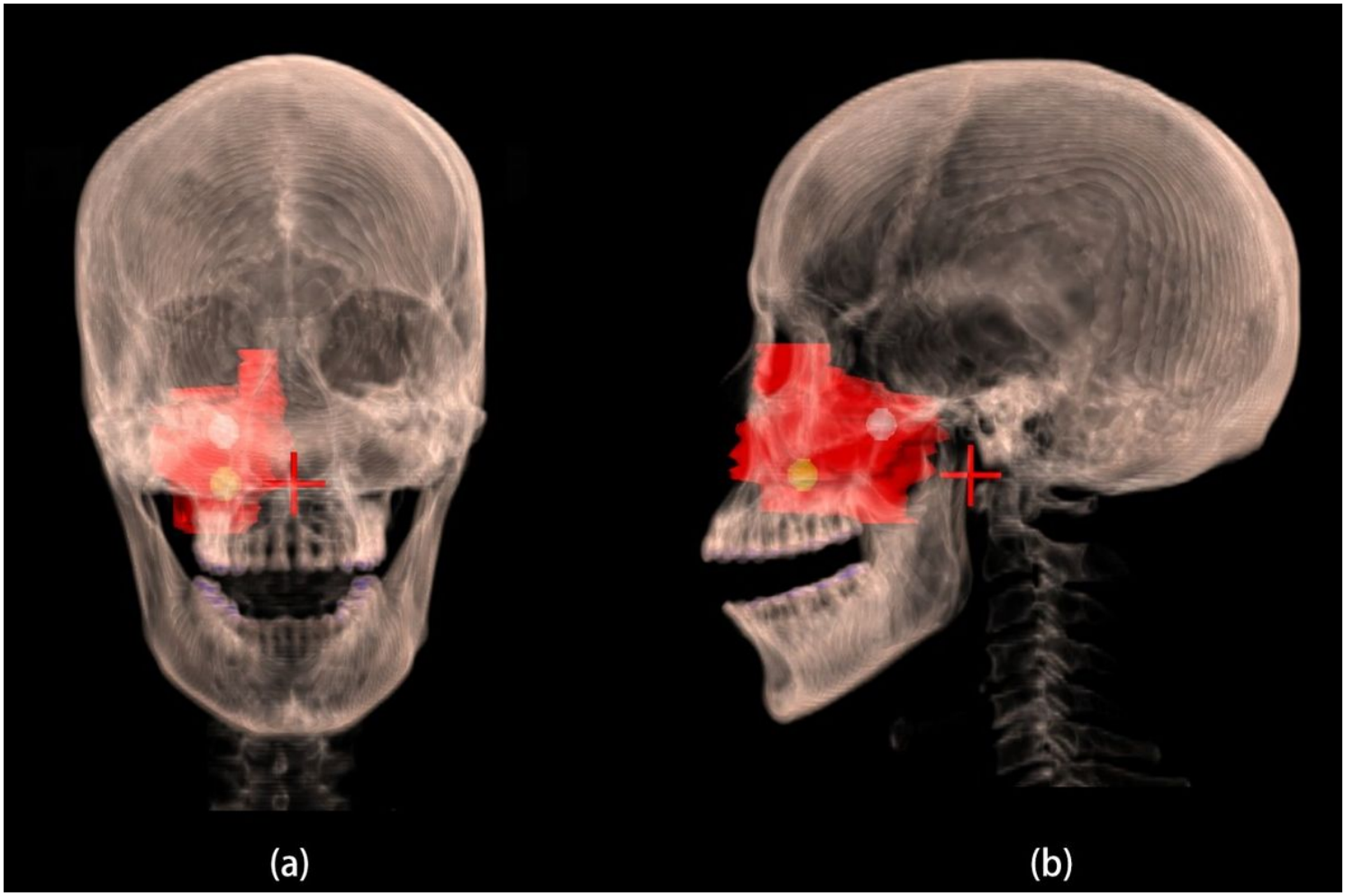

Figure 1

An example of vertex geometry within the GTV. Notes: The GTV is 72.64 cc, 2 vertices were deployed with a c-to-c distance of 3.04 cm. (a) Patterns in coronal view. (b) Patterns in sagittal view.

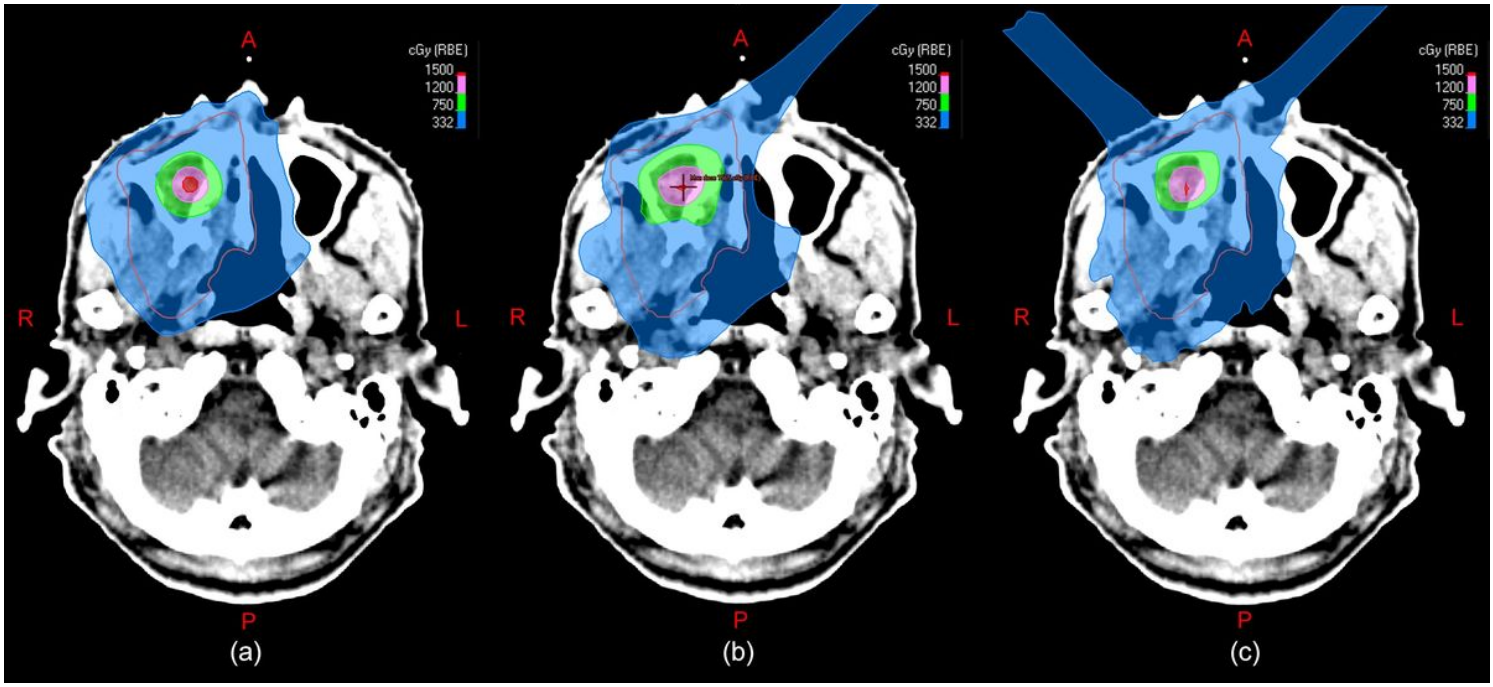

Figure 2

Comparison of dose distributions among photon, proton, and carbon ion LRT plans. Notes: This patient has a GTV of 72.64 cc, 2 vertices, and 3.04 cm centre-to-centre distance. The prescribed dose of the LRT plan was 15 Gy (RBE) to the vertices and 3.5 Gy (RBE) in one fraction to the periphery as CTVboost. (a) Dose distribution of photon LRT plan. (b) Dose distribution of proton LRT plan. (c) Dose distribution of carbon ion LRT plan

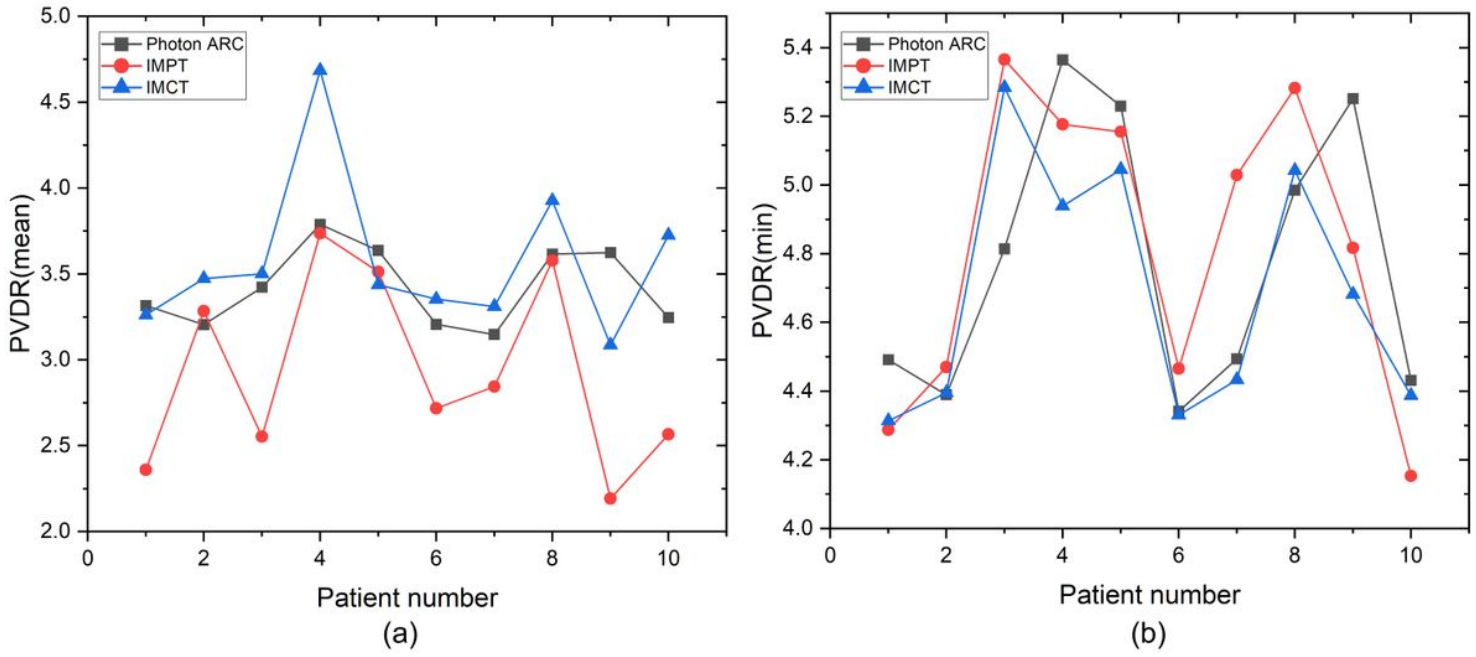

Figure 3

Comparison of PVDRmin and PVDRmean among IMCT, IMPT, and photon ARC plans. Notes: (a) Comparisons of PVDRmin; (b) Comparisons of PVDRmean